Bogie Frame Assessment: A Multibody Dynamic Approach

Thanaporn Talingthaisong[1] Aunna Sukhom[2] Sedthawatt Sucharitpwatskul[3]
Anchalee Manonukul[4] Panya Kansuwan[5*]

[1]*Department of Mechanical Engineering, Faculty of Engineering, Rajamangala University of Technology Isan Khon Kaen Campus, Khon Kaen, Thailand*
[2]*School of Mechanical Engineering, Institute of Engineering, Suranaree University of Technology, Nakhon Ratchasima, Thailand*
[3,4]*National Metal and Materials Technology Center, National Science and Technology Development Agency, Pathumthani, Thailand*
[5*]*Department of Mechanical Engineering, School of Engineering, King Mongkut's Institute of Technology Ladkrabang, Bangkok, Thailand*

*Corresponding Author. E-mail address: panya.ka@kmitl.ac.th

Received: 11 August 2024; Revised: 7 December 2024; Accepted: 27 December 2024
Published online: 27 June 2025

Abstract

Developing a new bogie frame design requires a complete design process to ensure the safe operation of the running vehicles. EN 13749 specifies the procedure from the initial design phase to the final verified on-track test. Due to the current power of computational hardware and software, the process can be performed and crossed over among phases seamlessly by integrating finite element analysis capability within multibody dynamic software. If design engineers perform the analysis entirely on computers before manufacturing the prototype, they can reduce product development time, which is the crucial benefit of optimizing their design. This paper presents the discrepancy of resulting stress from the calculation by the code with those from simulated test rigs within ADAMS. Furthermore, fatigue analysis software has demonstrated its effectiveness in evaluating fatigue life, particularly when considering the mean stress effect. The results can assist test engineers in locating hot spot positions for strain monitoring and further adjusting design procedures, especially for specific components such as side frames or cross beams.

***Keywords*:** ADAMS flex, Bogie frame, CAE fatigue, Durability, Multibody analysis

I. INTRODUCTION

National administrators financially support technology transfer in various industries to promote local industrial manufacturers. One of the major industries is the railway system, which results in railway engineering curriculums in many universities to produce working forces and railway organizations in various government sectors to administer and support activities to ensure continuous developments in the field. The technologies include fundamental research on railway vehicle dynamics [1] rail/wheel contact failure mechanism [2], [3] and track quality measurement and modification [4].

Manufacturing a new bogie frame design is challenging to qualify safety standards at higher operating velocities. Railway engineers must perform detailed calculations, control manufacturing quality, and validate the results at every step to conform to the standards. EN13749 and EN14363 by European standard body (CEN) are recognized. EN13749 specifies the complete design processes of a bogie frame, while EN14363 states the acceptance criteria of a railway vehicle via its running characteristics [5]–[7].

Previously, the design process for a new railway bogie frame depended on manufacturing experiences from on-bench static and fatigue tests according to UIC 515-1 for trailer bogies [8] UIC615-4 for motor bogies [9] and UIC 510-3 for freight bogies [10]. EN13749 now standardizes the acceptance process based on the results of structural calculations from static assessment and structural calculations from fatigue assessment. Further verification and validation tests are on-bench static, on-bench fatigue, and on-track tests.

The structural calculations for static and fatigue assessment use a well-accepted numerical method, i.e., the finite element analysis (FEA), to calculate the resulting stress. The force vectors and their applied location are predetermined theoretically from operational load cases (LCs). Typically, they deviate from on-bench and on-track tests due to different boundary conditions at the connection of the bogie frame with attached parts or equipment. Thus, the code requires verifying and validating the calculated stress with stress derived from attached strain gauges when the body frame is subjected to on-bench and on-track tests. The significant advantage of the on-bench and on-track tests is that we can measure the forces at attached equipment and thus its fatigue life.

Nevertheless, the suitable location to attach the strain gauge is still undetermined. Designers usually consult finite element analysis and multibody dynamics (MBD) to locate the positions. The on-bench test is necessary to assess the stress and force before assembling the train for the on-track test.

The last step of the complete design program is the on-track test. The test is formidable but inevitable if the bogie frame is the new design. According to the standard, manufacturers must perform twisted track tests and curve track tests on each test zone. One of the EN13749's objectives is the strain measurement. During the test, test engineers record, evaluate, and document the complete verification program to verify that there is no excessive plastic deformation during the test and no fatigue damage within an extrapolation method. If the bogie is an existing design bogie, reduced programs with only calculation and on-bench test programs are adequate.

Due to the development of multibody dynamics such as Automated Dynamic Analysis of Mechanical Systems (ADAMS), a widely used tool in the field, engineers simulate the dynamic behavior of mechanical systems under various loading conditions. ADAMS has proven effective in simulating bogie frame dynamics, facilitating the optimization of strain gauge placement during experimental tests [11]. Similarly, the integration of MBD with FEA has been successfully applied to refine bogie designs and predict structural durability under varying load conditions [12]. Engineers can reduce the product development time during the validation and

verification process. A virtual prototyping process using the software makes time reduction possible by building a model, testing the design, reviewing results, and finally improving the model through parameterized or optimized processes. When forces at each joint can be determined, we predict more precise loads and more accurate subsequent durability of the structure. In addition, the multibody dynamic with a flexible body approach suggests a high-stress location where the engineer should attach the strain gauges when the real on-bench test needs to be performed. In this paper, we compare stress using three different approaches: 1) finite element analysis using forces suggested in the code, 2) finite element analysis using forces at connecting joints from on-bench test simulated in ADAMS, and 3) finite element analysis using flexible body analysis from on-bench test simulated in ADAMS.

II. RESEARCH METHODOLOGY

A. Bogie Model Definition

According to EN13749, the bogie frame (figure 1a) is considered as category B-I for mainline and inter-city passenger carrying rolling stock application in Thailand. It comprises an S355J2W welded plate for two side frames and an S355J2H plate for the two cylindrical pipes joining the side frames. The mechanical properties of the materials are provided in table 1.

Table 2 demonstrates mass system parameters used for numerical analysis. For subsequent finite element analysis, the same meshed bogie frame is used with tet10 element type having an average mesh size of 15 mm, as shown in figure 1b.

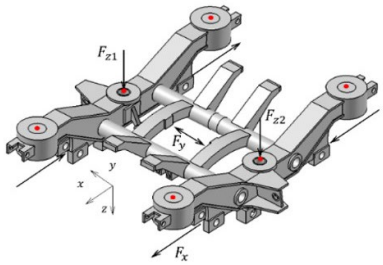

a) bogie frame geometry

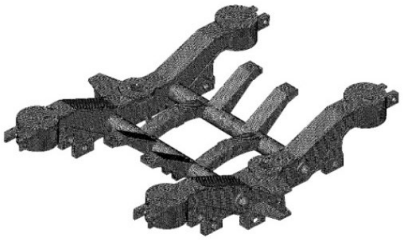

b) meshed geometry

Figure 1: a) bogie frame geometry b) meshed geometry

Table 1: Materials' mechanical properties

Properties	Value	Unit
Poisson's ratio	0.3	-
Elastic Modulus	207	GPa
0.2% Yield strength	355	MPa
Ultimate tension strength	600	MPa

Table 2: System parameters used for numerical analysis

Mass parameters	Symbol	Value	Unit
Vehicle mass	M_V	41490	kg
Exceptional design payload	P_1	10899	kg
Normal design payload	P_2	7930	kg
Bogie mass	m	5000	kg
Bogie mass without any secondary spring mass	m^+	4856	kg
Bogie frame mass	m_t	1485	kg
Moment of inertia of bogie frame in roll	I_{tx}	754	$kg \cdot m^2$
Moment of inertia of bogie frame in pitch	I_{ty}	683	$kg \cdot m^2$
Moment of inertia of bogie frame in yaw	I_{tz}	1375	$kg \cdot m^2$
Wheelset mass	m_w	932	kg
Moment of inertia of the wheelset – roll component	I_{wx}	272	$kg \cdot m^2$

Table 2: System parameters used for numerical analysis (Cont.)

Mass parameters	Symbol	Value	Unit
Moment of inertia of the wheelset – pitch component	I_{wy}	73	$kg \cdot m^2$
Moment of inertia of the wheelset – yaw component	I_{wz}	272	$kg \cdot m^2$
Primary vertical spring mass per piece		30	kg
Primary vertical damper mass per piece		20	kg
Secondary spring and damper mass per piece		42	kg
Secondary lateral damper mass per piece		11	kg
Secondary yaw damper mass per piece		18	kg
Axle box and arm per set		85	kg
Air compressor		450	kg
Anti-roll torsion bar per set		116	kg
Traction rod		96	kg
Traction seat		163	kg
Adjust mass bogie		160	kg
Adjust mass car body		616	kg
Dimension parameters			
Half of the track gauge	a	0.5000	m
Bogie frame wheel base	l	2.3000	m
Wheel radius	r_o	0.4255	m
Spring and damper parameters			
Primary suspension - Vertical stiffness	K_{wz}	9.95E05	N/m
Primary suspension – Vertical damping	C_{wz}	Figure 2a	
Secondary suspension – Vertical stiffness	K_{tz}	4.50E05	N/m
Secondary suspension – Vertical damping	C_{tz}	Figure 2b	
Secondary suspension – Yaw damping	C_{tx}	Figure 2c	
Secondary suspension – Lateral damping	C_{ty}	Figure 2d	

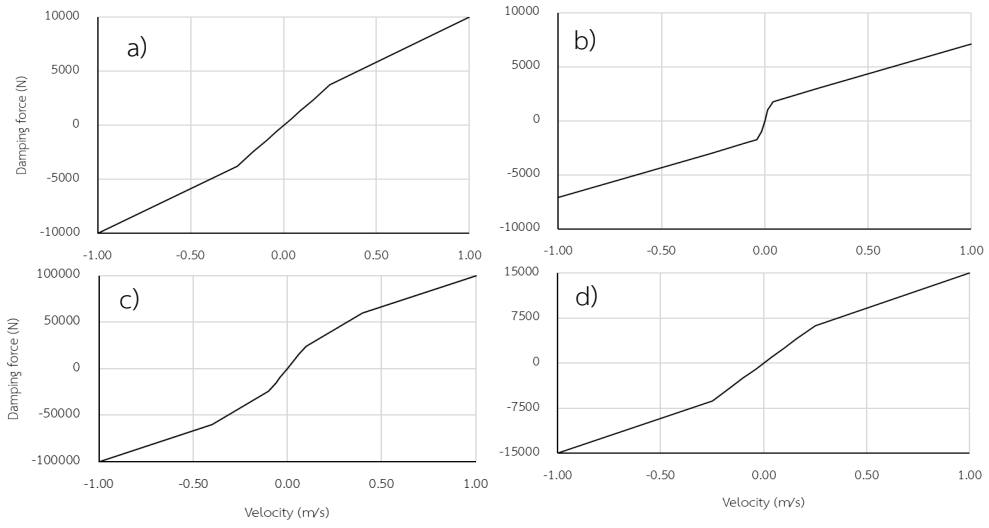

Figure 2: Damping coefficient curve

B. Structural Stress Analysis

There are two major computational assessments in the initial phase of the designing procedure, i.e., static stress analysis from exceptional loads and fatigue stress analysis from normal service loads [5]. In addition, we add a normal static LC. The three load categories are as follows.

1) Normal Static LC: This case considers only normal LC having two vertical forces ($F_{z1,2}$), in Eq. (1), applying on each side frame (figure 1a) with appropriate displacement constraints.

$$F_{z1} = F_{z2} = \frac{F_z}{2} = \frac{G(M_V+1.2P_2-2m^+)}{4} \quad (1)$$

2) Exceptional Static LCs: These loads are applied for static stress analysis to ensure limited plastic deformation in the frame and no exceeding critical forces at any attached equipment. The code requires four LCs combining vertical, transverse, longitudinal, longitudinal shunt, and twisted track forces.

Vertical force (F_z) derives from vehicle sprung mass, including design exceptional payload (P_1) with a vertical acceleration of 1.4 G as expressed in Eq. (2). According to EN 15663, P_1 is the summation of designed sitting and standing passenger mass, including their luggage.

$$F_{z1_{max}} = F_{z2_{max}} = \frac{F_{z_{max}}}{2} = \frac{1.4G(M_V+P_1-2m^+)}{4} \quad (2)$$

Transverse force (F_y) is the summation of lateral flange forces at wheel-rail contact patches when the vehicle negotiates a curve track. *Prud'homme* limit provides the formula for the contact force in Eq. (3).

$$F_{y1_{max}} = F_{y2_{max}} = \frac{F_{y_{max}}}{2} = 10^4 + \frac{(M_V+P_1)G}{12} \quad (3)$$

Other than the transverse force, when a vehicle passes a curve, longitudinal lozenging force (F_x) exist as in Eq. (4) to yaw the oppositely the bogie frame at each wheel.

$$F_{x1_{max}} = 0.1(F_{z_{max}} + m^+G) \quad (4)$$

Additionally, the damping coefficient curve illustrated in figure 2 corresponds to the data presented in table 2, which represents the relationship between velocity and damping force. The primary suspension's vertical damping is shown in figure 2(a), while the secondary suspension's vertical damping, yaw damping, and lateral damping are depicted in figures 2(b), 2(c), and 2(d), respectively.

Longitudinal shunt forces in the analysis equal the bogie inertia force under an acceleration of 3G. Finally, forces induced by a twisted track are considered in two cases, i.e., a track twisted 1% and a wheel completely unloaded. table 3 concludes the combination of the forces in each LC that the frame must pass the following regulation limit. The ratio of the 0.2% yield stress to the Von Mises stress in the whole structure is higher than 1 for the complete acceptance program and 1.5 for the reduced program.

Table 3: Force combination in each verified LC

Force type	LC01	LC02	LC03	LC04
Vertical force, $F_{z_{max}}$	✓	✓	✓	✓(*)
Transverse force, $F_{y_{max}}$	✓			
Longitudinal lozenging force, $F_{x1_{max}}$		✓		
Longitudinal shut load			✓	
Twisted loading	✓			
Wheel unloading				✓

**Empty Passenger Car*

3) Normal Fatigue LCs. The applied forces are the same as in exceptional loads but less severe. The vertical forces in Eq. (1) are sprung masses. Transverse forces on each axle are stated in Eq. (5), and longitudinal forces on each wheel are shown in Eq. (6). The twisted track to be assessed is at 0.5%.

$$F_{y1} = F_{y2} = \frac{F_y}{2} = \frac{F_y+m^+G}{8} \quad (5)$$

$$F_{x1} = 0.05(F_y + m^+G) \quad (6)$$

The static test corresponding to the combinations of vertical and transverse forces is defined by the 9 cases in table 4. Roll and bouncing, which induce quasi-static and dynamic variations of vertical forces, are represented by the coefficients α and β, respectively. Typically, the values of these coefficients are 0.1 and 0.2 for α and β, respectively.

Fatigue LCs corresponding to vertical, transversal, and twisted track forces are combined into different load cases in table 2, and the additional combined vertical and longitudinal load sequence in table 5.

Table 4: Vertical and transverse force combination

LCs	F_{z1}	F_{z2}	F_y	Twisted
1	$F_z/2$	$F_z/2$	0	✗
2	$(1+\alpha-\beta)F_z/2$	$(1-\alpha-\beta)F_z/2$	0	✗
3	$(1+\alpha-\beta)F_z/2$	$(1-\alpha-\beta)F_z/2$	F_y	✓
4	$(1+\alpha+\beta)F_z/2$	$(1-\alpha+\beta)F_z/2$	0	✗
5	$(1+\alpha+\beta)F_z/2$	$(1-\alpha+\beta)F_z/2$	F_y	✓
6	$(1-\alpha-\beta)F_z/2$	$(1+\alpha-\beta)F_z/2$	0	✗
7	$(1-\alpha-\beta)F_z/2$	$(1+\alpha-\beta)F_z/2$	$-F_y$	✓
8	$(1-\alpha+\beta)F_z/2$	$(1+\alpha+\beta)F_z/2$	0	✗
9	$(1-\alpha+\beta)F_z/2$	$(1+\alpha+\beta)F_z/2$	$-F_y$	✓

Table 5: Vertical and longitudinal force combination

LCs	F_{z1}	F_{z2}	F_x
1	$F_z/2$	$F_z/2$	0
2	$F_z/2$	$F_z/2$	F_{x1}
3	$F_z/2$	$F_z/2$	$-F_{x2}$

C. Boundary Conditions

The location of displacement boundary conditions in the calculation is expressed in table 6. The displacement boundary conditions in x-, y-, and z-directions in exceptional LCs are shown in table 6, in which the blank means no displacement constraint. There are no rotation constraints. For normal LCs, the displacement boundary condition is the same as LC03 in table 6. In all cases, the self-weight of the bogie frame is considered with gravitational acceleration (G) of 9806.65 mm/s^2

D. Test Rig Model

The complete approached program performs the strength verification on the bogie test rig to verify the static and fatigue calculation from the strain measurement at determined spots that experience high-stress values. The loading resembles static and fatigue calculation cases but includes forces at attached equipment joints. A simulated test rig is a model with attached equipment such as an anti-roll bar, secondary suspension, and passenger loads on top of a pivot plate. The frame is connected to four axle boxes via primary suspension systems and to a passenger car via secondary suspension systems. Suspension parameters are provided in table 2. As a result, a complete assembly of the bogie with an entire mass of 5000 kg is shown in figure 3.

Table 6: x-,y-,z-displacement constraint, <x, y, z>, for each exceptional LC

Force type	LC00	LC01	LC02	LC03	LC04
Front left spring	<0, ,0>	<0, ,-1.15>	< 0, ,0>	< , ,0>	< , , >
Front right spring	<0,0,0>	<0,0,0>	<0,0,0>	< , ,0>	<0,0,0>
Rear left spring	< , ,0>	< , ,1.15>	< , ,0>	< , ,0>	< , ,0>
Rear right spring	< ,0,0>	< ,0,0>	< , 0, 0>	< , ,0>	< ,0,0>
Second spring left	< , , >	< , , >	< , , >	<0,0, >	< , , >
Second spring right	< , , >	< , , >	< , , >	<0,0, >	< , , >

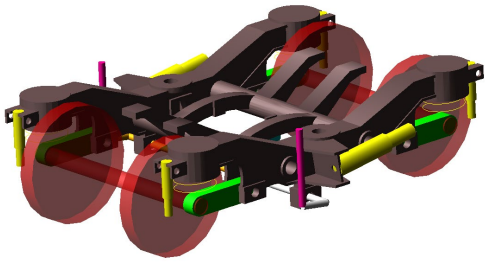

Figure 3: The bogie assembly.

E. Fatigue Strength Properties of the Materials

S-N curves can be approximately established on ultimate tension strength and elastic constant using a power relationship

$$S = 10^C N^b \quad (7)$$

In which S is stress, N is number of cycles, and C and b are material constants. Given the mechanical properties in table 1 with the derived parameter in table 7, the S-N curve of S355J2W is shown in figure 4.

Table 7: Fatigue strength properties of S355J2W

Parameter	Description	Value
SR1	Stress range at 1 cycles (MPa)	2726
SR1E6	Stress range at 1E6 cycles (MPa)	428
b1	First strength exponent	-0.1339

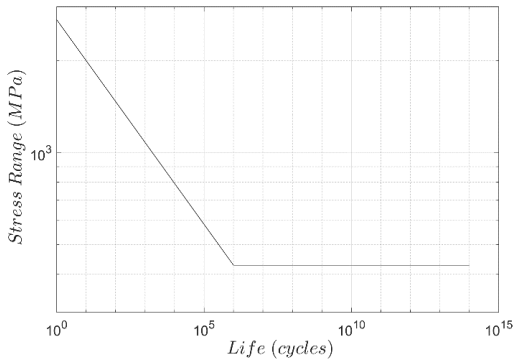

Figure 4: S-N curve

IV. RESULTS AND DISCUSSION

A. Normal Static LC

1) Finite Element Analysis Using Code Forces: From Eq. (1), the calculated normal force (F_Z) is 202478 N using normal payload (P_2) of 7930.19 kg. After we applied boundary conditions (LC00 as shown in table 6), the maximum Von Mises stress is 97.9 MPa occurring at the connection of the spring pocket with the frame, as shown in table 8.

2) Finite Element Analysis Using ADAMS-Derived Forces: The advantage of using multibody dynamics in the static LCs is the force determination at each joint (figure 3). The information allows us to calculate the resulting stress in the structure more precisely. To create a model resembling the above static analysis, we perform mass balance for an equivalent system to get the forces and moments at the following 21 locations (table 9). Their specific locations are demonstrated in figure 5. In this case, fixed x-, y-, and z-displacement boundary conditions are applied to the secondary suspension location on the side frames.

When the force from ADAMS on the FEA model is applied, the maximum Von Mises stress is 97.9 MPa at the same location as the above case, i.e., the connection of the spring pocket with the frame (table 8).

Table 8: Resulting Von Mises stress from LC00 using three different approaches

Description	FEA – code forces	FEA – ADAMS derived forces	FEA – Flex body analysis
Von Mises Stress	94.9 MPa	100.0 MPa	89.8 MPa
Location	Outer left of rear primary spring pocket	Outer left of rear primary spring pocket	Outer upper plate of the left side frame
Fringe plot	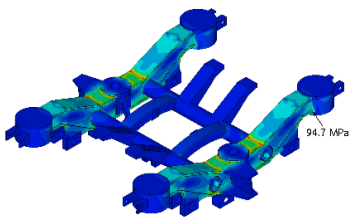	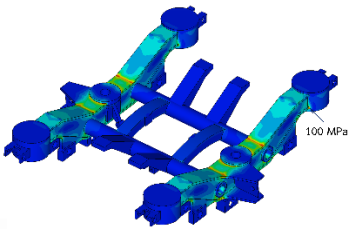	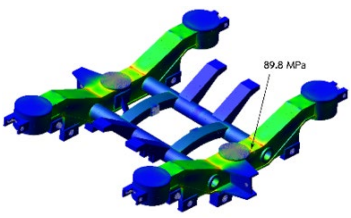

Table 9: Force location on the bogie frame

Position	Description
1, 2	Primary spring front left/right
3, 4	Primary spring rear left/right
5, 6	Primary vertical damper front left/right
7, 8	Primary vertical damper rear left/right

Table 9: Force location on the bogie frame (Cont.)

Position	Description
9, 10	Axle box front left/right
11, 12	Axle box rear left/right
13, 14	Anti roll bar left/right
15, 16	Secondary lateral damper left/right
17, 18	Secondary yaw damper left/right
19, 20	Secondary spring left/right
21	Traction rod to bogie frame

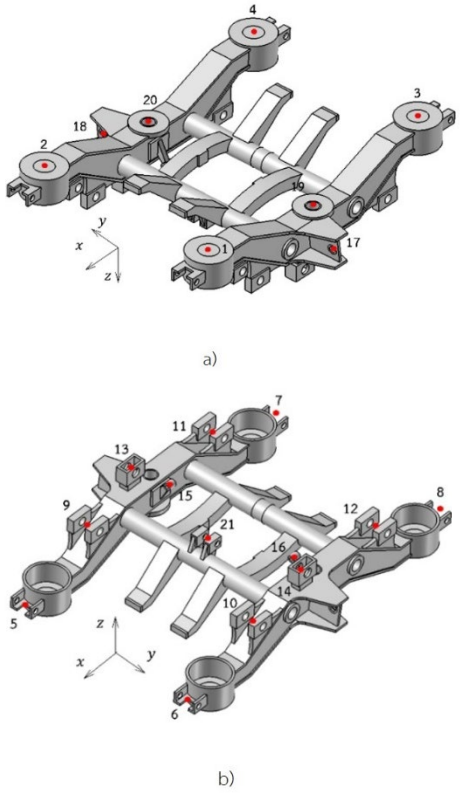

Figure 5: Applied force locations a) bottom view and b) top view.

3) Finite Element Analysis Using Flexible Body Analysis: ADAMS flex is based on modal theory to solve displacement problems in eq. (8) the result is valid if the linear superposition assumption is satisfied.

$$u = \sum_{i=1}^{M} q_i \, \emptyset_i \qquad (8)$$

in which u is the structural displacement, q_i is the linearized matrix, $\emptyset_i$ is the mode shape function, M is the number of modes in consideration. A flexible body frame in modal neutral file format was first generated in MSC.PATRAN using Craig Bampton method, the summation of constraint modes and fixed boundary normal modes. The flexible body replaces the rigid one on the simulated test rig in figure 3. We obtained the maximum Von mises stress at 89.8 MPa on the outer back of SS seat (table 8). The location is identified as the second maximum rank in the former two cases. Note that the initial modeling in ADAMS is a partial coupling that disables initial components 3, 4, 5, and 9 by default.

B. Exceptional Static LC

1) Finite Element Analysis Using Code Forces: From Eq. (2) to (4) and table 6, the force can be calculated (table 10) and applied at specific locations to obtain resulting stresses in table 11 using an exceptional payload (P_1) of 10899 kg. The result identifies a critical spot at the weld joint between connecting bar with side frames. The ratio of the 0.2% yield stress to the Von Mises resulting stress is 1.18. According to the code, the bogie frame is acceptable in the full program but in the reduced program.

Table 10: Calculated forces and loads

Parameter	Value	Unit
$F_{z1_{max}} = F_{z2_{max}}$	146481	N
$F_{z1_{empty}} = F_{z2_{empty}}$	109073	N
$F_{y1_{max}} = F_{y2_{max}}$	52813	N
$F_{x1_{max}} = F_{x2_{max}}$	34058	N

Table 11: Results of Von Mises stress for each exceptional LCs

Description	**LC11**	**LC12**
FEA – code forces		
Max. Von Mises stress	206 MPa	156 MPa
Location	Inner back of right SS seat	Outer left of rear primary spring pocket
Fringe plot	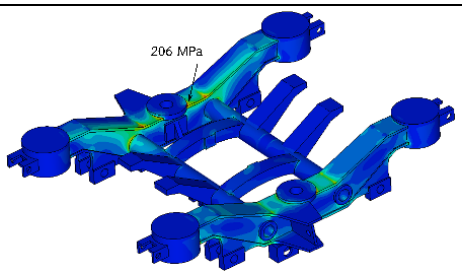	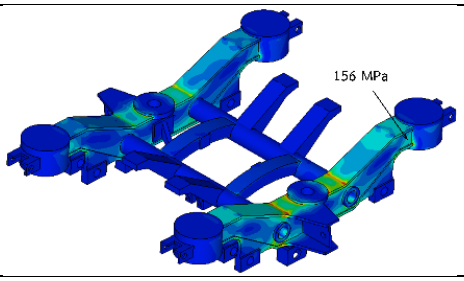
FEA – ADAMS derived forces		
Max. Von Mises stress	168 MPa	140 MPa
Location	Inner back of left SS seat	Outer left of rear primary spring pocket
Fringe plot	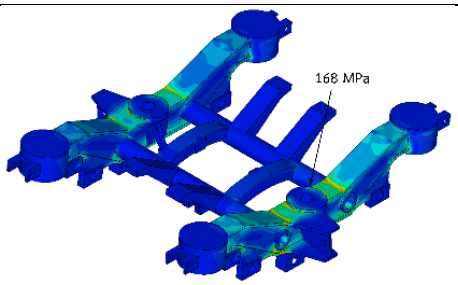	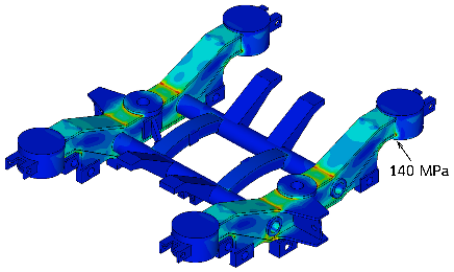
FEA – Flex body analysis		
Max. Von Mises stress	137 MPa	130 MPa
Location	Inner upper plate of the left side frame	Outer back of left SS seat
Fringe plot	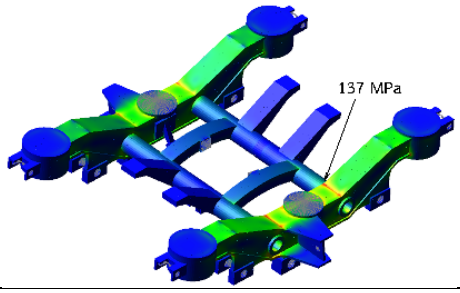	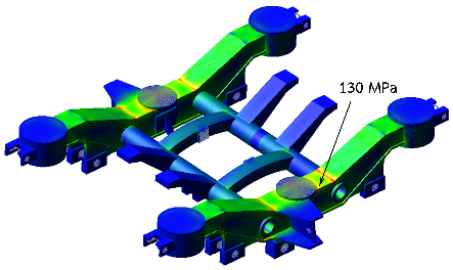
Description	**LC13**	**LC14**
FEA – code forces		
Max. Von Mises stress	140 MPa	301 MPa
Location	Inner back of right SS seat	Inner right of connecting bar
Fringe plot	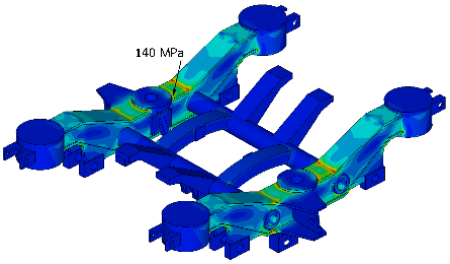	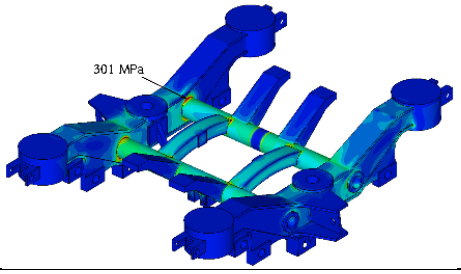

Table 11: Results of Von Mises stress for each exceptional LCs (Cont.)

Description	LC13	LC14
FEA – ADAMS derived forces		
Max. Von Mises stress	145 MPa	159 MPa
Location	Outer right of front primary spring pocket	Outer left of rear primary spring pocket
Fringe plot	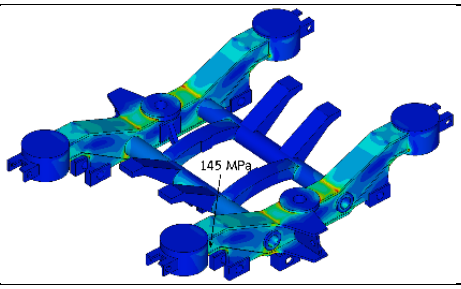	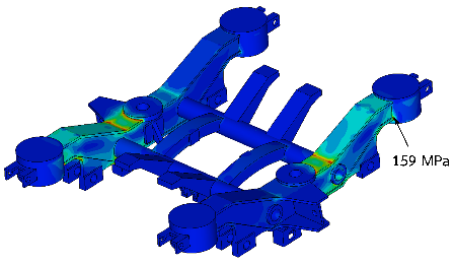
FEA – Flex body analysis		
Max. Von Mises stress	125 MPa	174 MPa
Location	Outer upper plate of the left side frame	anti-roll bars connecting plate
Fringe plot	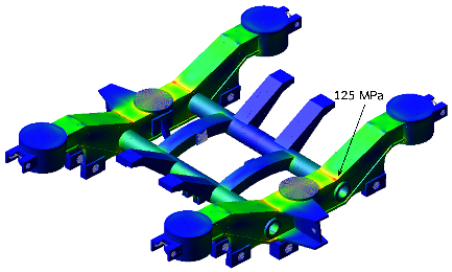	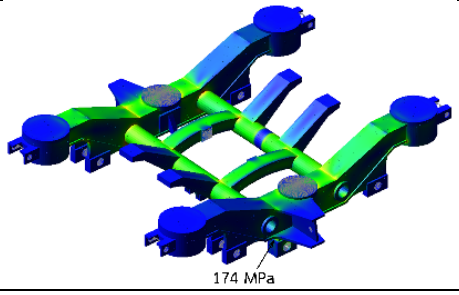

2) Finite Element Analysis Based on Resulting Forces Obtained from ADAMS: As in the previous case of static normal load case, resulting forces at each connection from the rigid multibody calculation are applied to the meshed bogie frame at which dead weight is attached to using 0D mass element. We used 50% sprung mass and 50% unsprung mass for components in the primary suspension system figure 3. The resulting stress and hot spot locations in each case are shown in table 11. When using this type of analysis, the maximum stress occurs in LC11 instead of LC14.

3) Finite Element Analysis Using Flexible Body: The maximum stresses in this type of analysis occur in LC14 but at different locations, i.e., the anti-roll bar support connection to the bogie frame. The behavior could not be captured in other analyses. The flexible frame body reacts with a rigid bar and induces a moment at the support. This makes the shift of the hot spot location in the case.

It is obvious from the above results that inconsistent stress is associated with hot spot locations. Nevertheless, actual strain measurement must be conducted to verify the critical location from the results. In all cases, using the code forces is the most conservative analysis compared with other methods.

C. Normal Fatigue LC

1) Finite element analysis using code force: In this approach, we proposed fatigue-life analysis of the load cases stated in table 4 and table 5 simultaneously under static vertical loading, bouncing, and curve negotiate loading. Eight cases are identified as shown in table 12 with a loading sequence in figure 6 and figure 7.

Table 12: Quasi-static loading and result stress

LCs	Description	Number of cycles in a block load	Stress amplitude (MPa)
1	Normal static load	Static case	94.6 (mean)
2	Rolling	1	9.07
3	Bouncing	30	18.2
4	Fx	1	5.84
5	Twist track on left turn	0.5	2.45
6	Twist track on Right turn	0.5	2.36
7	Lateral load on Left turn	0.5	68.0
8	Lateral load on Right turn	0.5	68.0

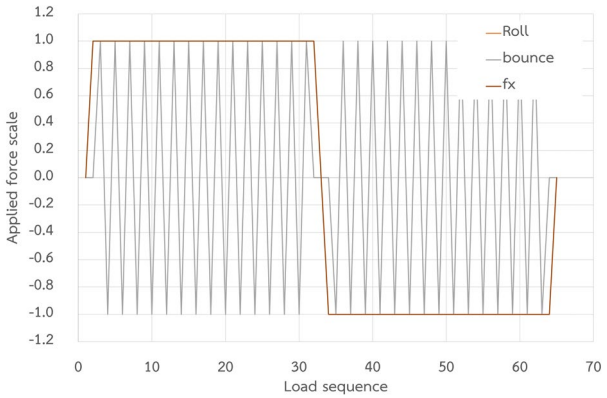

Figure 6: Loading sequence for LC 2, 3, and 4.

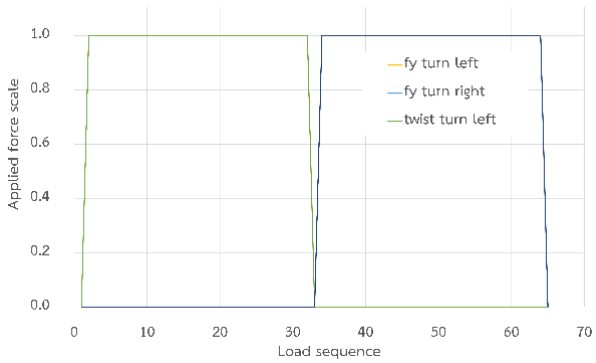

Figure 7: Loading sequence for LC 5, 6, 7, and 8

The accumulated damage due to combined stress at different time steps results in an infinite fatigue life when we consider the mean stress effect according to Goodman equation. The stress results from each load case are presented in table 12, and the fatigue life from CAE fatigue 2024.1.1 is shown in figure 8.

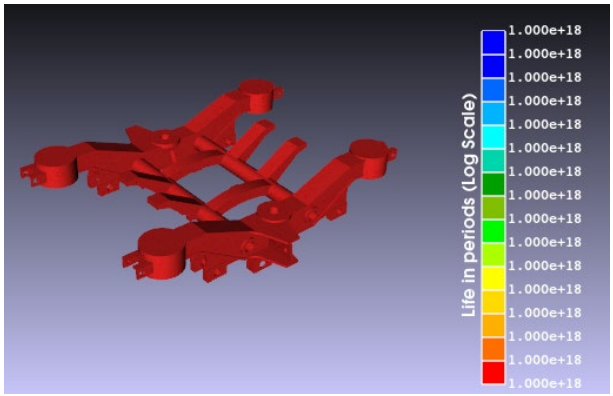

Figure 8: Fatigue life cycles, a quasi-static fatigue test.

The critical locations are identified at the anti-roll bar connection to the frame and the primary spring housing to the frame (figure 11). Nevertheless, the stress variation is in the range of 124-128 MPa which results in infinite life in accordance with the results from CAE fatigue 2024.1.1 under Goodman criteria.

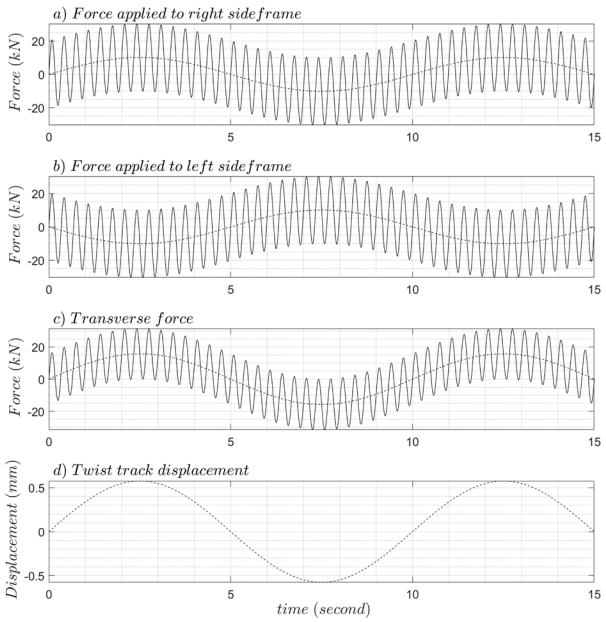

Figure 9: Applied fatigue loading profiles.

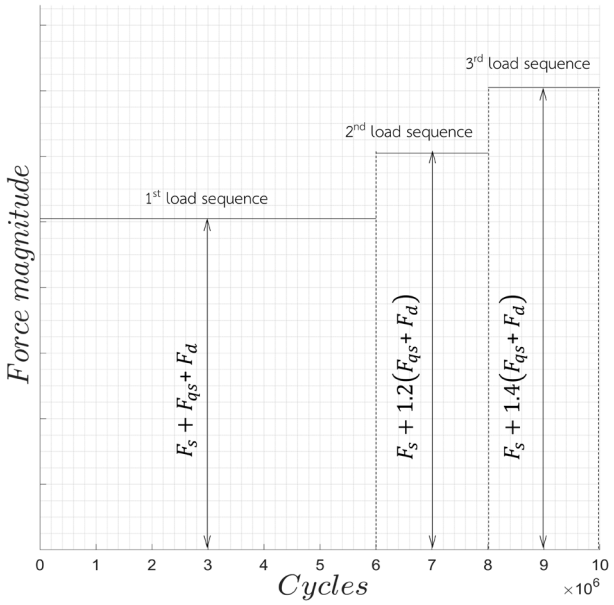

Figure 10: Fatigue loading sequences.

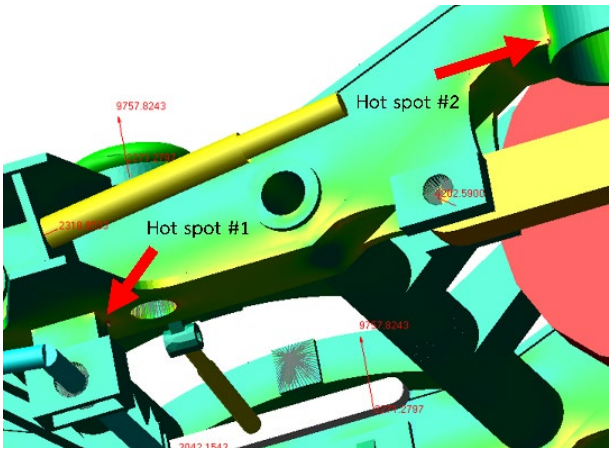

Figure 11: Critical stress locations.

V. CONCLUSION

A complete assessment of a passenger bogie is demonstrated by comparing the direct finite element approach and the multibody dynamic approach. The latter approach provides profound identification of critical locations.

In the normal static load case, a multi-body dynamic approach with a flex body results in the lowest stress level. On the contrary, the location of critical stress is different from the results of the others. The conclusions are the same in exceptional load cases. This indicates that further validation of strain measurement might be necessary to certain results.

Fatigue analysis software has proven usefulness in evaluating fatigue life assessments when considering mean stress effect. Stress in each loading scenario resulting from finite element analysis is suitable for simple loading conditions, as in the case of static fatigue test rigs. For more complicated real loading, we should resort to CAE fatigue. Both approaches provide infinite fatigue life in our cases.

ACKNOWLEDGEMENT

This work (P1950662) is supported by Research Development Innovation Management for National Strategic and Network Division, National Science and Technology Development Agency, Thailand.

REFERENCES

[1] T. Talingthaisong, S. Sucharitpwatskul, A. Manonukul, and P. Kansuwan, “Sensitivity analysis of suspension parameters of the critical velocity of a railway bogie on a tangent track using standardized regression coefficients,” *J. Eng. Digit. Technol. (JEDT)*, vol. 11, no. 1, pp. 88–98, 2023.

[2] N. Tosangthum *et al.* “Dry rolling-sliding wear behavior of ER9 wheel and R260 rail couple under different operating conditions,” *Wear*, vol. 518–519, Apr. 2023, Art. no. 204636, doi: 10.1016/j.wear.2023.204636.

[3] A. Sukhom, T. Talingthaisong, S. Sucharitpwatskul, A. Manonukul, and P. Kansuwan, “Study of rolling contact fatigue mechanism of ER9 and R260 wheel/rail materials,” in *Proc. 13th TSME Int. Conf. Mech. Eng. (TSME-ICoME)*, Chiang Mai, Thailand, Dec. 12–15, 2023, pp. 1–10.

[4] P. Kansuwan, S. Sucharitpwatskul, and A. Manonukul, “Application of fast fourier transform to the synthesis of track irregularities,” in *Proc. 8th Int. Conf. Eng., Appl. Sci. Technol. (ICEAST)*, Chiang Mai, Thailand, Jun. 2022, pp. 1–10.

[5] *Railway applications - Wheelsets and bogies - Method of specifying the structural requirements of bogie frames*, EN 13749:2011, European Committee for Standardization (CEN), Brussels, Belgium, Mar. 2011.

[6] *Railway applications - Testing for the acceptance of running characteristics of railway vehicles - Testing of running behaviour and stationary tests*, EN 14363:2005, European Committee for Standardization (CEN), Brussels, Belgium, Jun. 2005.

[7] G. Mancini and A. Cera "Design of railway bogies in compliance with new EN 13749 European standard," presented at the 7th World Congr. Railway Res. (WCRR), Montréal, Canada, Jun. 4–8, 2006.

[8] *Passenger rolling stock - Trailer bogies - Running gear - General provisions applicable to the components of trailers bogies*, UIC Code 515-1, International Union of Railways, Paris, France, 2003.

[9] *Motive power units - Bogies and running gear - Bogie frame structure strength tests*, UIC Code 615-4, International Union of Railways, Paris, France, 1994.

[10] *Wagons - Strength testing of 2 and 3-Axle bogies on test rig*, UIC Code 510-3, International Union of Railways, Paris, France, 1989.

[11] A. Ibrahim, M. A. Abdullah, and K. Hudha, "Multibody dynamics models of railway vehicle using ADAMS/Rail," *Appl. Mechanics Mater.,* vol. 393, pp. 644–648, Sep. 2013.

[12] E. Zhang, C. L. Pun, A. Hiew, and W. Yan, "Dynamic response and wear analysis of a swing nose crossing in heavy haul railways," *Railway Eng. Sci.*, vol. 33, pp. 192–215, 2025.